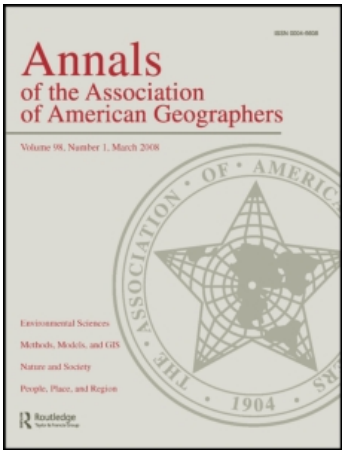

Annals of the Association of American Geographers

Publication details, including instructions for authors and subscription information:
http://www.informaworld.com/smpp/title~content=t788352614

Comparison of Three Maps at Multiple Resolutions: A Case Study of Land Change Simulation in Cho Don District, Vietnam

Robert Gilmore Pontius Jr.[a]; Smitha Peethambaram[b]; Jean-Christophe Castella[c]
[a] School of Geography, Clark University, [b] Mactec Engineering and Consulting, [c] Institut de Recherche pour le Développement (IRD) and Centre for International Forestry Research (CIFOR),

First published on: 27 October 2010

To cite this Article Pontius Jr., Robert Gilmore , Peethambaram, Smitha and Castella, Jean-Christophe(2011) 'Comparison of Three Maps at Multiple Resolutions: A Case Study of Land Change Simulation in Cho Don District, Vietnam', Annals of the Association of American Geographers, 101: 1, 45 — 62, First published on: 27 October 2010 (iFirst)
To link to this Article: DOI: 10.1080/00045608.2010.517742
URL: http://dx.doi.org/10.1080/00045608.2010.517742

Comparison of Three Maps at Multiple Resolutions: A Case Study of Land Change Simulation in Cho Don District, Vietnam

Robert Gilmore Pontius, Jr.,* Smitha Peethambaram,† and Jean-Christophe Castella‡

*School of Geography, Clark University
†Mactec Engineering and Consulting
‡Institut de Recherche pour le Développement (IRD) and Centre for International Forestry Research (CIFOR)

Geographic modelers frequently compare maps of observed land transitions to maps of simulated land transitions to relate the patterns in reference maps to the output from a simulation model. Pixel-by-pixel analysis of raster maps at a single resolution is useful for this task at a single scale, but scientists often need to consider additional scales. This article presents methods to satisfy this need by proposing a multiple-resolution method to compare land categories in three maps: a reference map of time 1, a reference map of time 2, and a simulation map of time 2. The method generates a three-dimensional table that gives the percentage of the study area for each combination of categories at the maps' native resolution and at several nested sets of coarser squares. The method differentiates allocation disagreement within coarse squares, allocation disagreement among coarse squares, quantity disagreement, and agreement. We illustrate the method with output from a run of the SAMBA agent-based model from 1990 to 2001 using 32-m resolution pixels for Cho Don District, Vietnam. Results show that half of the overall disagreement is attributable to allocation disagreement within squares that are 506 m × 506 m, which is about the average size of a village. Much of the remaining disagreement is misallocation of forest and shrub between the northern and southern parts of the district, which is caused by differences between the data and the simulation concerning transitions from the crop and shrub categories. *Key Words: accuracy, category, GIS, model, scale.*

研究地理模型的学者们经常需要把实际观察到的土地类型转化地图和模拟的土地类型转化地图进行对比，从而得以将参考地图上的模式和模型模拟的结果进行相关映射。对于此项任务，在单一的尺度上，对单一分辨率的栅格地图进行单个像素的点对点分析是有用的，但是，科学家往往需要考虑其它的尺度。本文介绍了能够满足该任务需求的若干方法，提出了一种土地类别的多重分辨率方法，并被用来比较下述三种地图：时间 1 的参考地图，时间 2 的参考地图，以及时间 2 的模拟图。该方法生成了一个三维表，给出了在原始分辨率地图和多个嵌套的更粗糙分辨率的样方区地图上研究区每个类别的各自百分比例。在粗分样本方区内部和粗分样本方区之间，该方法可以用于定位类别差异，并可以对类别差异和类别相似度进行数量化分析。我们对该方法通过下述实例进行了说明：试验区选定为越南的赵唐区，利用 SAMBA 基于代理的模型，使用了 1990 年至 2001 的 32 米分辨率的像素分析。结果表明，在粗分样本方区的 506 米分辨率下，一半左右的整体类别差异可以由此获得，这个尺度大概是一个村庄的平均面积。其余的类别差异被错误地定位，大部分属于该地区北部和南部的森林和灌木，这是由于观测时间不同而造成的差异，并且和模拟过程中涉及到的从作物到灌木类别的转化处理有关。*关键词：精度，类别，地理信息系统，模型，尺度。*

Quienes diseñan los modelos geográficos frecuentemente comparan los mapas de transiciones observadas en la tierra con mapas de transiciones simuladas de tierras para relacionar los patrones en mapas de referencia con el producto de un modelo de simulación. El análisis pixel por pixel de mapas *raster* a resolución única es útil para esta tarea a una sola escala, aunque a menudo los científicos necesitan considerar escalas adicionales. En este artículo se presentan métodos para satisfacer esta necesidad proponiendo uno de resolución múltiple para comparar categorías de tipos de tierras en tres mapas: un mapa de referencia de tiempo 1, un mapa de referencia de tiempo 2 y un mapa de simulación de tiempo 2. El método genera una tabla tridimensional que suministra el porcentaje del área de estudio para cada combinación de categorías a la resolución nativa de los mapas y a varios conjuntos empaquetados de cuadrados menos ajustados. El método diferencia la distribución de desconformidad dentro de los cuadrados sin ajuste, la distribución de desconformidad entre tal tipo de cuadrados, la cantidad de desconformidad, y la conformidad. Ilustramos el método con lo que se obtiene al ejecutar el modelo SAMBA

Annals of the Association of American Geographers, 101(1) 2011, pp. 45–62
Initial submission, August 2008; revised submissions, June and December 2009; final acceptance, February 2010
Published by Taylor & Francis, LLC.

basado en agentes de 1990 a 2001, usando una resolución de pixeles de 32-m en el Distrito de Cho Don, Vietnam. Los resultados muestran que la mitad de la desconformidad total se atribuye a la distribución de la desconformidad dentro de cuadrados de 506 m x 506 m, lo cual es aproximadamente el tamaño promedio de una aldea. Mucho de la restante desconformidad es la asignación equivocada de bosque y monte entre las partes norte y sur del distrito, causada por diferencias entre los datos y la simulación relacionada con las transiciones entre las categorías de cultivos y monte. *Palabras clave: exactitud, categoría, GIS, modelo, escala.*

For several types of applications, scientists need to compare three maps that show the same categorical variable of a single study area. This is especially true for measuring the output of models that simulate change among land categories from an initial time to a subsequent time on a raster grid of pixels (Pontius et al. 2008). In this context, a reference map of time 1, called reference t1, shows the land categories at the initial time, a reference t2 map shows the land categories at the subsequent time, and a simulation t2 map shows the simulated land categories at the subsequent time. This article uses the maps in Figure 1 as a case study, where the pixels' native resolution is 32 m.

The three possible two-map comparisons can be helpful because comparison of reference t1 and reference t2 indicates the observed transitions, comparison between reference t1 and simulation t2 indicates the simulated transitions, and comparison between reference t2 and simulation t2 indicates the simulation's agreement and disagreement with the data at time 2. A two-dimensional contingency table, or cross-tabulation matrix, is a popular way to summarize the information of a two-map comparison, especially because the two-dimensional table can serve as the basis for a variety of summary statistics (Fielding and Bell 1997; Stehman 1997; Congalton and Green 1999; Alo and Pontius 2008). Initially, it is tempting to try to examine the relationships among the three maps by computing the three possible two-map comparisons, but these three pairwise comparisons have substantial limitations. For example, the matrix of observed transitions might show that a pixel transitioned from category A to category B, and the matrix of simulated transitions might show that a pixel transitioned from category A to category B, but the pairwise matrices do not indicate whether these pixels coincide. The three-dimensional table solves this problem efficiently, because the three-dimensional table simultaneously documents the observed transition and the simulated transition for each pixel. This characteristic enables the three-dimensional table to serve as the basis for more types of statistical analysis than the pairwise matrices can. Specifically, the three-dimensional table reveals how much of the agreement between reference t2 and simulation t2 is attributable to land persistence versus land change. It also reveals how much of the disagreement between reference t2 and simulation t2 is due to an imperfectly simulated quantity of each transition versus an imperfectly simulated spatial allocation of each transition. Figure 2 helps to visualize the three-dimensional space that a three-dimensional table occupies, illustrated for four categories. In general, if there are J categories, then the three-dimensional table will have J^3 entries within the table and additional entries on the outer edges indicating the marginal totals that give the two-map comparisons.

If all of the pixels contain exactly one category, then pixel-by-pixel computation of the two-dimensional and the three-dimensional tables is straightforward, because the position of each pixel registers entirely in exactly one entry in the table. When the table is calculated for the entire study area, each entry indicates the number of pixels that have the particular combination of categories in the study area. It is common to divide all the entries by the total number of pixels to produce results that are proportions that sum to one.

Pixel-by-pixel analysis at the data's native resolution fails to consider the spatial allocation of the types of disagreement. For the purposes of this article's proposed method, let us define minor allocation disagreement as the type of disagreement where the maps differ by category at a particular pixel's position in the raster at the native resolution, and the matching category exists within a coarser square neighborhood to which the pixel belongs. In other words, minor allocation disagreement is the allocation disagreement that occurs among pixels that are within coarse squares that partition the map into clusters of pixels. Major allocation disagreement occurs where the maps differ by category at a particular pixel's position in the raster at the native resolution and the matching category does not exist within the coarser square neighborhood to which the pixel belongs but does exist outside of the coarser square. That is, major allocation disagreement is the allocation disagreement that occurs among coarse squares. It is important to distinguish minor from major allocation disagreement, because it can be useful to interpret minor allocation disagreement differently than major allocation

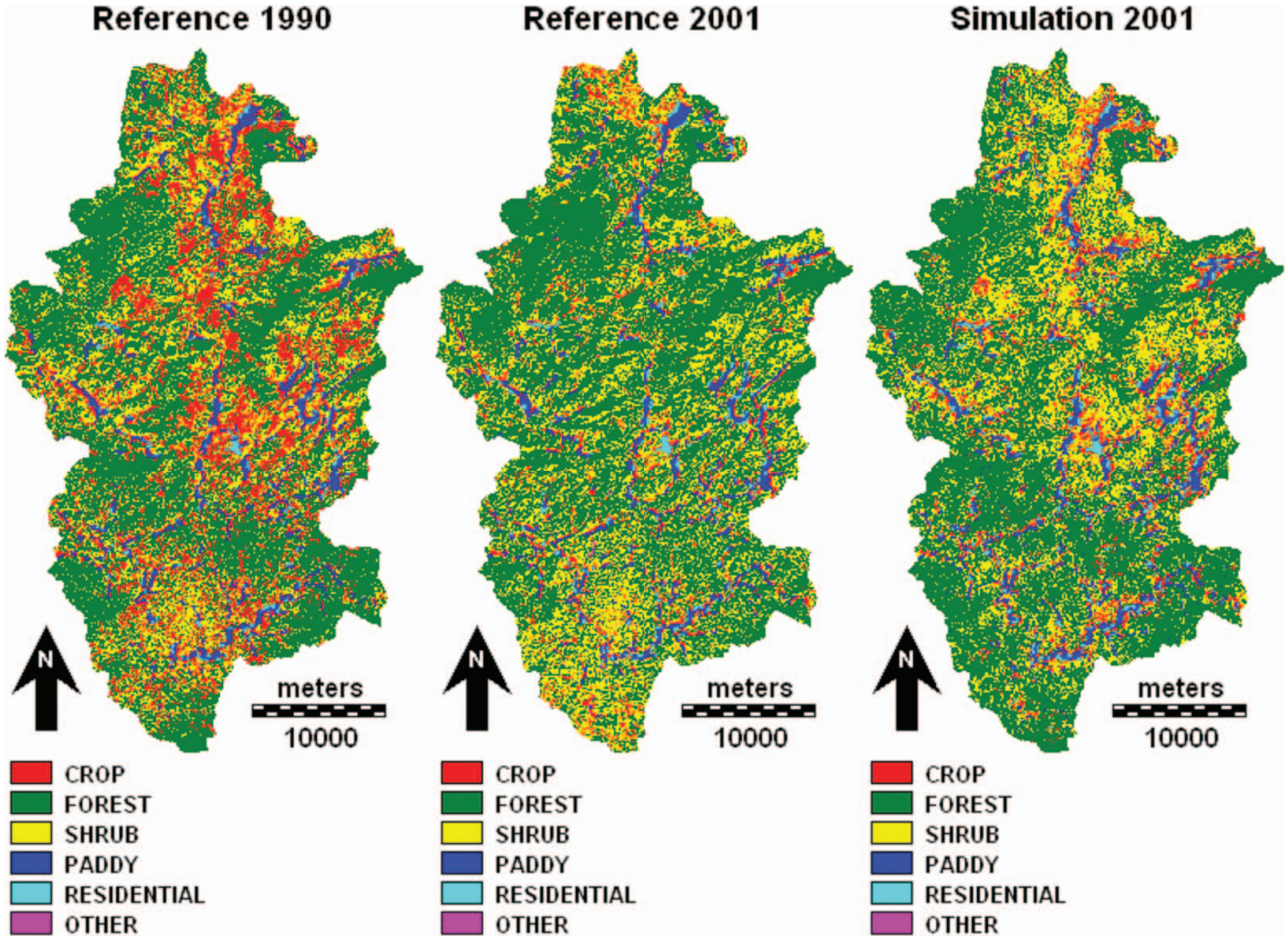

Figure 1. Three maps for the case study of Cho Don District, Vietnam (Castella, Tronche, and Nguyen 2002; Castella, Trung, and Boissau 2005).

disagreement for practical applications. It is usually less important to know whether a simulation matches the allocation of the categories at the data's native resolution than whether a simulation matches the quantity of each category within coarser areal units in the study area, especially when the native resolution is dictated by factors, such as the resolution of the remote sensing device, that are not related to the practical research question. Furthermore, possible errors in the reference maps might cause disagreement in the three-map comparison, but if these errors are sufficiently minor to be considered correct for practical purposes, it is helpful to have a method that gives an option to consider minor allocation disagreement to be agreement. Moreover, the cause of the minor disagreement can be different than the cause of the major allocation disagreement, in which case it is helpful to have a quantitative method to separate minor from major allocation disagreement.

This article uses multiple-resolution analysis to distinguish minor allocation disagreement from major allocation disagreement. Multiple-resolution analysis compares maps at the native resolution and at several coarser resolutions by computing the proportion of each category that coarse squares contain. The method considers minor allocation disagreement to be agreement and major allocation disagreement to be disagreement. Multiple-resolution analysis examines several coarser resolutions; thus, it analyzes multiple definitions of minor, because minor means within a coarse square.

The coarsening of the resolution introduces a major mathematical challenge. When pixels are converted to coarser resolutions, the coarse squares can contain positive proportions to more than one category. In this situation, it is not immediately clear how to compute the table, because there can be a seemingly infinite number of potentially reasonable ways to distribute the entries within the table when a coarse square has partial membership to multiple categories (Binaghi et al. 1999; Lewis and Brown 2001; Latifovic and Olthof 2004;

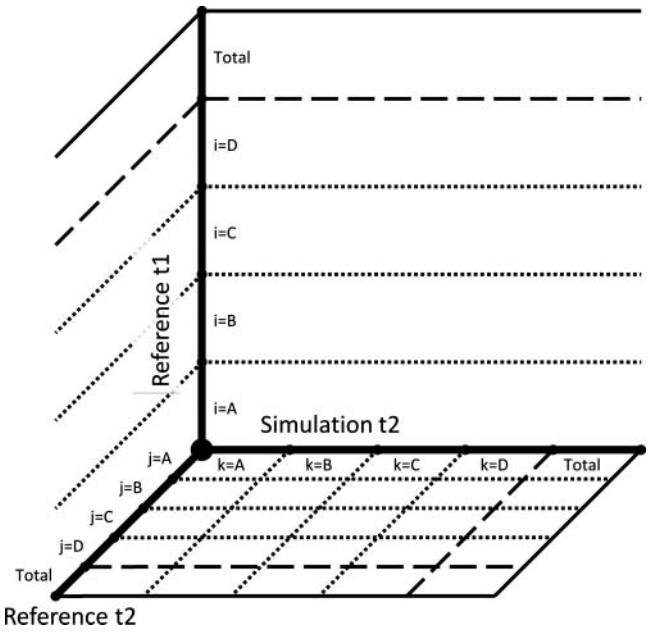

Figure 2. Space for the three-dimensional table that compares reference t1, reference t2, and simulation t2.

Fisher et al. 2006; Silván-Cárdenas and Wang 2008; Pontius and Connors 2009). The method to construct the table should derive from the specific goal of the analysis.

The major goal of this article is to present a method to construct a three-dimensional table for a study area that is partitioned into areal units that contain proportions of multiple categories. We construct the table such that its entries are proportions of the study area that sum to one and its marginal totals sum to the proportions of the categories in the maps. These characteristics allow us to interpret each entry in the table as the proportion of the study area that posses a particular combination of categories in reference t1, reference t2, and simulation t2. Therefore, we can use the three-dimensional table to perform multiple-resolution analysis in a manner that is interpretable for practical applications because it distinguishes minor allocation disagreement within coarse areal units from major allocation disagreement among coarse areal units.

This problem is important, as evidenced by the tremendous number of publications concerning how variation in scale influences map properties and measures of association (Bian 1997; Cao and Lam 1997; Goodchild and Quattrochi 1997; Collins and Woodcock 1999; Marceau 1999; Atkinson and Tate 2000; Dietzel and Clarke 2004; Lam et al. 2004; Wu 2004; Kuzera and Pontius 2008). There have also been many proposed methods to compare maps that have mixed, soft, or fuzzy classified pixels (Townsend 2000; Woodcock and Gopal 2000; Okeke and Karnieli 2006; Stehman et al. 2007; Gómez, Biging, and Montero 2008). This article addresses these issues through comparison among three maps, whereas other methods focus on comparisons between two maps (Foody 2002; Visser and de Nijs 2005; Csillag and Boots 2006; Pontius et al. 2007). This article is the culmination of a series of articles that address scale and mixed pixels in the context of map comparison. Pontius (2002) proposed a method to compare two maps that contain mixed pixels in a manner that budgets the disagreement in terms of two separable components, quantity disagreement and allocation disagreement. Pontius, Huffaker, and Denman (2004) showed how to use those concepts to measure the accuracy of a land change model at multiple resolutions via a pair of two-map comparisons. Pontius and Cheuk (2006) gave equations to calculate a composite matrix, which is a two-dimensional table for comparing two maps that have mixed pixels. The composite matrix is particularly useful for multiple-resolution analysis because it treats minor allocation disagreement as agreement (Kuzera and Pontius 2008; Pontius and Connors 2009). This article builds on these concepts to perform a three-map comparison by computing a three-dimensional table in a manner that is consistent with the composite matrix.

Methods

Data

Cho Don Case Study. We illustrate the concepts with a case study in Cho Don, Vietnam. Castella et al. (2005; Castella, Trung, and Boissau 2005) provided the data from their agent-based land change modeling project called SAMBA. Figure 1 shows six categories for all three maps on the same raster grid, where each pixel belongs to exactly one category and is 32 m × 32 m. The underlying remotely sensed image dictates this native resolution. The crop category refers to upland crop and the paddy category refers to wetland paddy. Reference t1 is the most accurate map available for 1990, reference t2 is the most accurate map available for 2001, and simulation t2 is the output from the SAMBA simulation model for 2001.

For this case study, the SAMBA model simulates land transitions from 1990 to 2001, which marks a decade of major land reforms that accompanied the decollectivization of agriculture in Vietnam (Castella et al. 2006). These reforms had a tremendous impact on

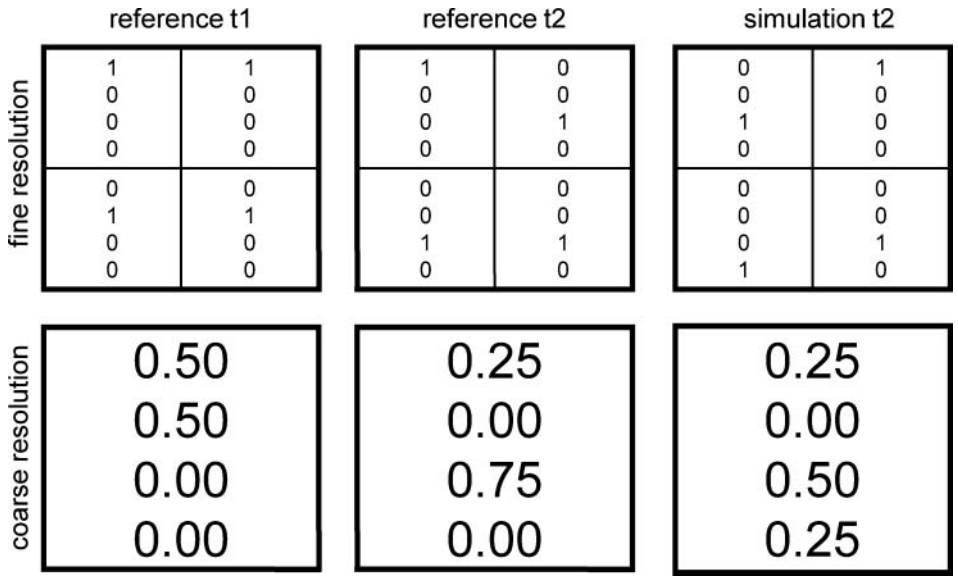

Figure 3. Example maps at fine resolution in top row and at coarse resolution in bottom row showing membership within the squares ordered from top to bottom for four categories: A, B, C, and D.

land use in the upland areas. These rapid institutional changes were concomitant with a phenomenon known as *forest transition*, which is a phase of heavy deforestation that subsequently leads to forest regeneration (Meyfroidt and Lambin 2008). The SAMBA model was developed to explore the causal relations between land reforms and the forest transition by explicitly representing household decisions related to land management and their impact on land use conversion. The model simulates village-level land use changes based on the modeled behavior of individual households and then aggregates the simulated maps from the village level to the district. The model's assumptions concerning household behavior derive from refined field research and participatory modeling methods (Castella, Trung, and Boissau 2005). The purpose of the land use simulations was to examine at the broad district level research hypotheses that were based on more detailed village-level case studies. The simulations were meant to guide land use planning at the district level.

Visual comparison between reference 1990 and the other two maps in Figure 1 shows substantial observed and simulated loss of crop. Comparison between reference 2001 and simulation 2001 shows that most of the disagreement in the north is observed forest that is simulated as shrub, whereas most of the disagreement in the south is observed shrub that is simulated as forest.

This article uses a three-dimensional table to quantify the agreement and disagreement among these three maps at multiple resolutions. The next section presents the fundamental ideas using a simplified example.

Simple Example. Figure 3 gives an example that is useful to consider when working through the mathematics to construct the table. At each resolution, there are three maps called reference t1, reference t2, and simulation t2. Each of the three maps in the top row gives information for four pixels at the fine resolution. The four numbers within each pixel are ordered from top to bottom to denote the pixel's proportion of categories A, B, C, and D, respectively. At the fine resolution, each pixel belongs completely to the single category denoted by the placement of the 1 among the four numbers in the pixel. The maps demonstrate common types of situations that simulation modelers encounter. The pixel in the upper left shows the observed transition is from A to A, but the simulated transition is from A to C. The pixel in the upper right shows the observed transition is from A to C, but the simulated transition is from A to A. Thus, both pixels register as disagreement at the fine resolution because the simulation misallocated transitions between neighboring pixels. The pixel in the lower left shows an observed transition from B to C, but the simulation is from B to D. The pixel in the lower right shows both observed and simulated transitions from B to C. Thus, three of the four pixels show disagreement at the fine resolution. Each of the three maps in the bottom row is a coarse-resolution version of the map immediately above it, so that each coarse map consists of exactly one pixel. The proportion of each category in the coarse square is the average of the native resolution pixels that constitute the coarse square; therefore, coarse squares can have positive proportions for more than one category and the proportions

in each coarse square sum to one. The remainder of this section uses this example to illustrate details of the mathematics.

Notation for Multiple Resolutions

This article uses the following mathematical notation:

G = maximum index for grain of resolution where the entire study area is in one square.
g = index for grain of resolution = $1, \ldots, G$.
Ng = number of coarse squares at resolution g.
n_g = index for coarse square at resolution $g = 1, \ldots, Ng$.
J = number of categories.
i, j, k = indexes for categories = $1, \ldots, J$.
Qin_g = proportion of category i in square n_g in reference time 1 map.
Rjn_g = proportion of category j in square n_g in reference time 2 map.
Skn_g = proportion of category k in square n_g in simulation time 2 map.
$Tijkn_g$ = entry in three-dimensional table that corresponds to category i in reference time 1, category j in reference time 2, and category k in simulation time 2 for square n_g.
$Uijk_g$ = entry in three-dimensional table that corresponds to category i in reference time 1, category j in reference time 2, and category k in simulation time 2 for entire study area at resolution g.
Wn_g = weight for square n_g.

The resolution of the native pixels is the grain index $g = 1$. At this native resolution, $Wn_1 = 1$ denotes the weight for each pixel in the study area, and $Wn_1 = 0$ denotes the weight for each pixel not in the study area. The pixels with weight of zero are masked from the analysis, which is necessary for nonrectangular study areas. The weight for a coarse square is the average of the weights of the native resolution pixels that constitute the coarse square. In this manner, the weight for each coarse square is the proportion of the coarse square that resides in the study area, so coarse squares that are completely in the study area have a weight of one, whereas coarse squares that are partially in the study area have a positive weight of less than one. For each coarse square that is partially in the study area, the proportion of each category is calculated as the average from the contributing native resolution pixels. For example, if a coarse square consists of four native resolution pixels where the first pixel belongs to category A, the second pixel belongs to category B, the third pixel belongs to category C, and the fourth pixel is out of the study area, then the coarse square has a weight of 3/4 and has a proportion of 1/3 to each category A, B, and C. This approach allows the method to work for study areas that are not rectangular, including areas that are not contiguous.

The upper left corner of the raster is the starting point for our algorithm that aggregates pixels to convert the map from the native resolution to coarser resolutions, as is typical of geographic information system (GIS) software. All the resolutions have this same starting point; therefore, each set of smaller squares is nested within a set of larger squares. Selection of the starting point dictates how the coarse squares partition the study area. If the aggregation were to start at a different point, then the resulting coarse squares would partition the map into different subregions. Thus, the starting point of the aggregation influences the definition of minor, because minor means within coarse squares. This article's Discussion section relates this characteristic to the modifiable areal unit problem (Openshaw 1984) and gives advice concerning how to use this characteristic as an advantage during interpretation of the results.

Three-Dimensional Table

Strategy to Compute Entries. Figure 4 revisits the space that the three-dimensional table occupies. For a single square n_g, the marginal totals along the outer edges of the space show the $3 \times J$ boxes that record the proportions of the categories within square n_g for reference t1, reference t2, and simulation t2 (i.e., Qin_g, Rjn_g, and Skn_g). The challenge is to fill the J^3 entries within the table so that each marginal total equals the sum of the entries in the corresponding plane that passes through the space. There could be a large number of solutions to this challenge, depending on the values of Qin_g, Rjn_g, and Skn_g. This article presents a method to satisfy its specific goal of distinguishing minor allocation disagreement from major allocation disagreement, because the method's equations uniquely satisfy the rules in Table 1.

Table 1 gives four ordered rules to construct the values of the entries in the three-dimensional table for a single square, regardless of whether the square contains exactly one category or contains positive proportions to more than one category. Rule 1 maximizes the total agreement between reference t2 and simulation t2 within each square, by assuming the greatest possible intersection among matching categories in reference

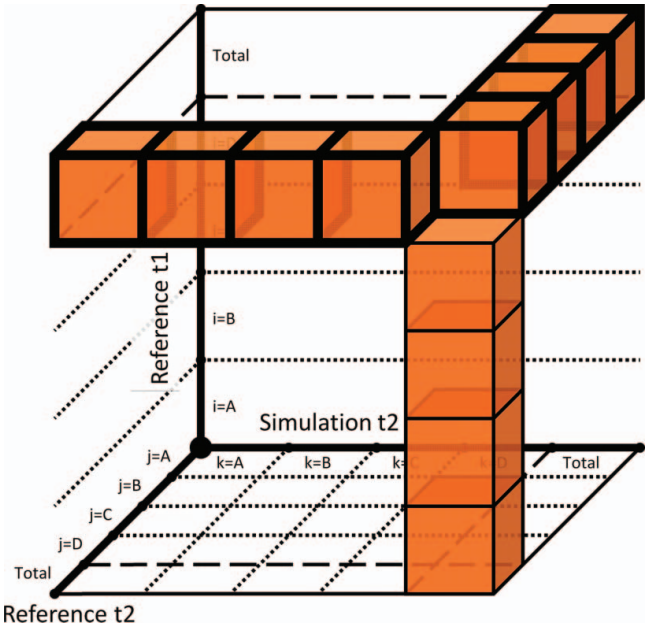

Figure 4. Marginal totals on the three outer edges of the three-dimensional table. These totals are the proportions of categories in reference t1, reference t2, and simulation t2. Figure 4 is available in color online.

Table 2. Three-dimensional table for example maps at fine resolution, where layers for A and B are reference t1

			Simulation t2				
		Reference t1	A	B	C	D	**Total**
Reference t2	A	A			0.25		**0.25**
		B					
		Total			**0.25**		**0.25**
	B	A					
		B					
		Total					
	C	A	0.25				**0.25**
		B			0.25	0.25	**0.50**
		Total	**0.25**		**0.25**	**0.25**	**0.75**
	D	A					
		B					
		Total					
	Total	**A**	**0.25**		**0.25**		**0.50**
		B			**0.25**	**0.25**	**0.50**
		Total	**0.25**		**0.50**	**0.25**	**1.00**

Note: The entire table is zero for layers C and D for Reference t1, so those layers are not included. Blank entries are zeroes. Entries in bold are marginal totals.

t2 and simulation t2. Rule 2 maximizes agreement due to correctly simulated persistence within each square, by assuming the greatest possible intersection among matching categories in reference t1, reference t2, and simulation t2. Each subsequent rule computes the other entries in the table, conditional on how the previous rules allocate the proportions of the categories. Rule 3 quantifies the particular transition of correctly simulated change from t1 to t2, for entries where reference t2 agrees with simulation t2 but disagrees with reference t1. Rule 4 computes the remaining entries for which reference t2 disagrees with simulation t2.

For the example maps of Figure 2, Table 2 gives the results for the fine resolution and Table 3 gives the results for the coarse resolution. All zero entries are blank for ease of reading. Both tables have zeroes for layers C and D of reference t1, so the tables do not include those layers. The calculation of the entries in Table 2 is straightforward. We tally the number of pixels for each entry and then compute proportions by dividing all entries by the total number of pixels in the study area. In the example, each of the four pixels registers as 0.25 in exactly one entry in Table 2.

The next subsection describes a four-step process to compute the entries in Table 3, which requires more thought than for the fine resolution case because coarse squares can have positive proportions for multiple categories. The overall approach is to compute an entire three-dimensional table for each square and then to compute a weighted average of those tables to obtain a three-dimensional table for the study area.

Vertical Plane of Agreement between Reference t2 and Simulation t2. Figure 5 shows the vertical plane

Table 1. Ordered rules to construct the entries in the three-dimensional table for a single square that contains positive proportions of more than one category

1. Assign the greatest possible values to the table's marginal totals that indicate agreement between reference t2 and simulation t2, given the proportions of the categories within the square for reference t2 and simulation t2.
2. Assign the greatest possible values to the table's entries that indicate persistence simulated correctly, given the proportions of the categories within the square for reference t1, reference t2, and simulation t2.
3. Assign values to the table's entries that indicate change simulated correctly, by distributing the values in direct relation to the proportions of the categories in reference t1, given the proportions that were assigned by Rule 1 but were unassigned by Rule 2.
4. Assign values to the table's remaining entries by distributing the values in direct relation to the proportions of the categories in reference t1, reference t2, and simulation t2, given the proportions that were unassigned by Rules 1–3.

Table 3. Three-dimensional table for example maps at coarse resolution in same layout as Table 2

			Simulation t2				
		Reference t1	A	B	C	D	Total
Reference t2	A	A	0.25				**0.25**
		B					
		Total	**0.25**				**0.25**
	B	A					
		B					
		Total					
	C	A			0.167	0.083	**0.25**
		B			0.333	0.167	**0.50**
		Total			**0.50**	**0.25**	**0.75**
	D	A					
		B					
		Total					
	Total	**A**	**0.25**		**0.167**	**0.083**	**0.50**
		B			**0.333**	**0.167**	**0.50**
		Total	**0.25**		**0.50**	**0.25**	**1.00**

Note: The entire table is zero for layers C and D for Reference t1, so those layers are not included. Blank entries are zeroes. Entries in bold are marginal totals.

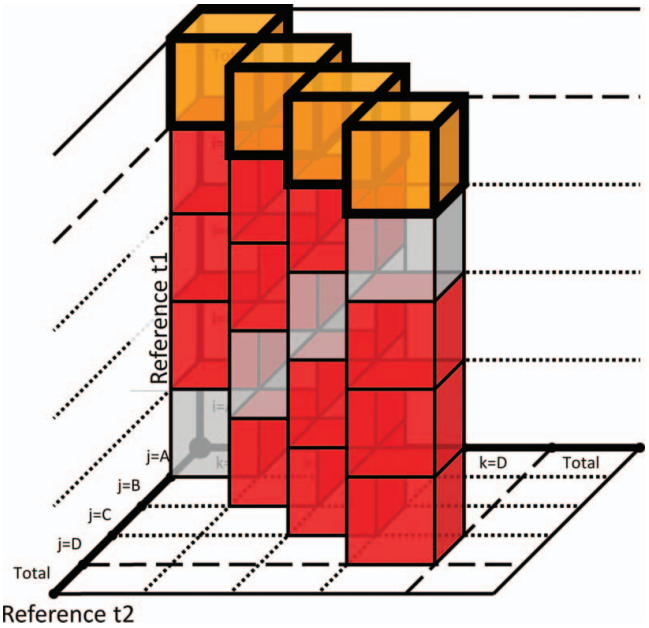

Figure 5. Entries on the vertical plane of agreement between reference t2 and simulation t2, including the marginal totals at the top. Figure 5 is available in color online.

where the table records agreement between reference t2 and simulation t2. The boxes outlined in bold at the top of this vertical plane give the marginal totals, where the marginal total for category j equals the sum of the boxes directly beneath it. The first step to construct the table for square n_g is to apply rule 1 to compute these marginal totals at the top of the vertical plane. Equation 1 performs this calculation in a manner consistent with the two-dimensional composite matrix of Pontius and Cheuk (2006). The right side of Equation 1 gives the marginal total that shows the agreement between reference t2 and simulation t2 for category j, and the left side of Equation 1 gives the sum of the entries that constitute this marginal total for category j. Equation 1 satisfies Rule 1, because Equation 1 computes minor allocation disagreement within a coarse square as agreement by assuming the greatest possible spatial intersection within each coarse square between matching categories for reference t2 and simulation t2. The minimum function defines this greatest possible intersection for each category j because the greatest possible intersection is constrained by the smaller of the proportions for category j in reference t2 and simulation t2 (Pontius 2002; Pontius and Connors 2009). The formula assures that if the native resolution pixels show allocation disagreement within a coarse square, then this disagreement counts as agreement within the coarse square. This occurs when categories in reference t2 and simulation t2 do not match at the native resolution but matching categories exist in native resolution pixels that are nearby, where nearby means within the coarse square.

$$\sum_{i=1}^{J} Tijjn_g = MIN(Rjn_g, Sjn_g) \qquad (1)$$

The second step to construct the table is to apply Rule 2 to compute the main diagonal within the vertical plane in Figure 5. Each entry for category j on the main diagonal indicates the proportion of square n_g for which all three maps agree on category j. Therefore, these J entries on the main diagonal are interpreted as persistence simulated correctly and are a subset of the total agreement between reference t2 and simulation t2. Equation 2 computes the values for these entries in a manner that satisfies Rule 2. Equation 2 treats minor allocation disagreement within a coarse square as agreement by assuming the greatest possible spatial intersection within each coarse square among matching categories for reference t1, reference t2, and simulation t2. As in Equation 1, the minimum function defines this greatest possible intersection within each coarse square for category j because the greatest possible intersection is constrained by the smallest proportion for category j among reference t1, reference t2, and

simulation t2.

$$Tjjjn_g = MIN(Qjn_g, Rjn_g, Sjn_g) \quad (2)$$

Rule 3 produces values in the vertical plane for the remaining entries that show change simulated correctly, which are the entries where reference t2 agrees with simulation t2 but disagrees with reference t1. Equation 3 satisfies Rule 3 by using multiplication to distribute the correctly simulated gross gain of category j among the categories that are not j in reference t1, as shown in each vertical stack of $J - 1$ boxes in Figure 5. The expression in square brackets to the left of the multiplication sign in Equation 3 is the correctly simulated gross gain of category j, expressed as the agreement between reference t2 and simulation t2 for category j minus the correctly simulated persistence for category j. The expression in square brackets to the right of the multiplication sign in Equation 3 is a weight for category i that distributes the correctly simulated gain of category j among the categories in reference t1. These weights exclude the correctly simulated persistence from reference t1 by the subtraction of $Tiiin_g$. The weights allocate the correctly simulated gross gain of category j among the categories in reference t1, because one is the sum of the weights over all categories i for which $i \neq j$.

$$Tijjn_g = \left[\left(\sum_{i=1}^{J} Tijjn_g\right) - Tjjjn_g\right] \times \left[\frac{(Qin_g - Tiiin_g)}{\sum_{i=1}^{J}(Qin_g - Tiiin_g)}\right] \quad \text{for } i \neq j \quad (3)$$

For our worked example at the coarse resolution, Equation 1 computes agreement for category A as 0.25 and agreement for category C as 0.50. Consequently, the total agreement between reference t2 and simulation t2 rises from 0.25 at the fine resolution to 0.75 at the coarse resolution, because the misallocation between two neighboring fine-resolution pixels becomes resolved as resolution becomes coarser. Equation 2 computes the correctly simulated persistence of category A as 0.25. Equation 3 distributes the 0.50 agreement for category C to the other categories in reference t1, by allocating 0.167 to category A and 0.333 to category B. One third of 0.5 is allocated to A, and two thirds of 0.5 is allocated to B, because one third and two thirds are the weights of categories A and B, respectively, in the expression to the right of the multiplication sign in Equation 3. These weights are the relative sizes of categories A and B in reference t1 that remain after a value of 0.25 for persistence simulated correctly is subtracted from reference t1.

Disagreement between Reference t2 and Simulation t2. Rule 4 completes the three-dimensional table by defining the entries that are not on the vertical plane of Figure 5. Equations 4 through 7 combine to satisfy Rule 4. The right side of Equation 4 takes the proportion of category i in reference t1 (Qin_g) and subtracts the proportions that Equations 1 through 3 allocated to the vertical plane in Figure 5. Thus, $Q'in_g$ is the remaining quantity of category i in square n_g for reference t1, which must be allocated among the entries that are not on the vertical plane of agreement between reference t2 and simulation t2. Equations 5 and 6 perform the same type of calculations for reference t2 and simulation t2, respectively, so $R'jn_g$ is the remaining quantity of category j in square n_g for reference t2, and $S'kn_g$ is the remaining quantity of category k in square n_g for simulation t2, after Equations 1 through 3 have determined the vertical plane of Figure 5. $Q'in_g$, $R'jn_g$, and $S'kn_g$ must be allocated among the entries that are not on the vertical plane. This allocation must satisfy the condition that the sum of the entries within the table equals the marginal totals (Qin_g, Rjn_g, Skn_g), which are along the outer edges of the space in Figure 4. Equation 7 accomplishes this allocation. The expression in square brackets to the left of the multiplication sign in Equation 7 assures that the sum of all entries in the table equals one, because the expression is one minus the sum of the entries in the vertical plane. The expression in the square brackets to the right of the multiplication sign in Equation 7 is a weight that performs the allocation in a manner consistent with Rule 4. The weights allocate all of the disagreement between reference t2 and simulation t2, because one equals the sum of the weights over all category combinations for which $j \neq k$. Finally, Equation 8 computes the table for the entire map by averaging the entries for all individual squares.

$$Q'in_g = Qin_g - \sum_{j=1}^{J} Tijjn_g \quad (4)$$

$$R'jn_g = Rjn_g - \sum_{i=1}^{J} Tijjn_g \quad (5)$$

$$S'kn_g = Skn_g - \sum_{i=1}^{J} Tikkn_g \quad (6)$$

$$Tijkn_g = \left[1 - \sum_{j=1}^{J}\sum_{i=1}^{J} Tijjn_g\right] \times \left[\frac{(Q'in_g \times R'jn_g \times S'kn_g)}{\sum_{i=1}^{J}\sum_{j=1}^{J}\sum_{k=1}^{J}(Q'in_g \times R'jn_g \times S'kn_g)}\right] \text{for} j \neq k \quad (7)$$

$$Uijk_g = \frac{\sum_{n=1}^{Ng}(Wn_g \times Tijkn_g)}{\sum_{n=1}^{Ng} Wn_g} \quad (8)$$

For our worked example using the single coarse square, Equation 4 produces $Q'A1_2 = 0.083$ and $Q'B1_2 = 0.167$. Equation 5 produces $R'C1_2 = 0.25$ and Equation 6 produces $S'D1_2 = 0.25$. Then Equation 7 allocates the 0.25 of disagreement between reference t2 and simulation t2 to produce $TACD1_2 = 0.083$ and $TBCD1_2 = 0.167$. The method can produce transitions at a coarse resolution that do not exist at a finer resolution. In the example, the combination where reference t1 is A, reference t2 is C, and simulation t2 is D does not exist at the fine resolution, but the combination exists in the table at the coarse resolution. This demonstrates how precise allocation information is strategically ignored as resolution becomes coarser.

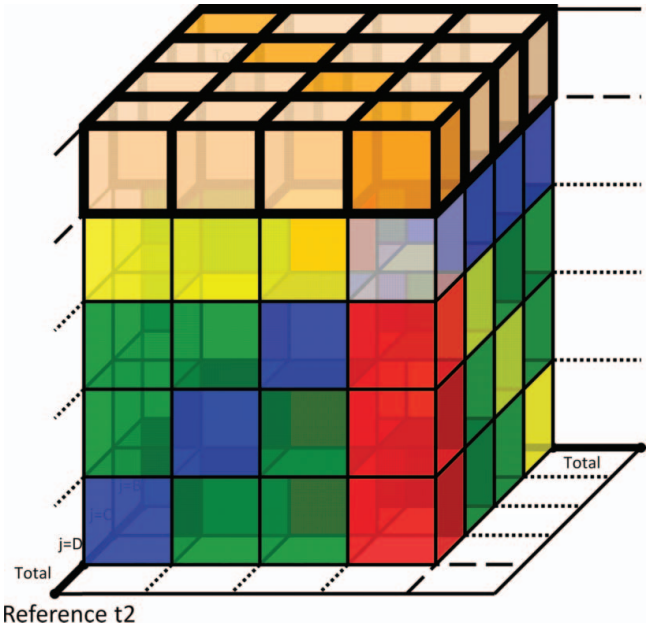

Figure 6. All entries within the three-dimensional table. The marginal totals at the top form the composite matrix that compares reference t2 and simulation t2. Figure 6 is available in color online.

Components of Agreement and Disagreement

Figure 6 shows all J^3 entries in the entire table. In addition, the top layer of marginal totals in Figure 6 is the composite matrix that compares reference t2 and simulation t2. It is helpful to associate each entry in the table with one of five interpretable components that sum to 100 percent of the study area. There are two components of agreement and three components of disagreement. Each component is color-coded in the digital version of this article. Persistence simulated correctly is the first component of agreement, which consists of the main diagonal of the table shown in gray. Change simulated correctly is the second component of agreement, which consists of the additional entries in the vertical plane of Figure 5 shown in red. All other entries show disagreement between reference t2 and simulation t2, and they can be separated into three types of disagreement. Persistence simulated as change consists of the entries where reference t1 matches reference t2 but does not match simulation t2, shown in yellow. Change simulated as persistence consists of the entries where reference t1 matches simulation t2 but does not match reference t2, shown in blue. Change simulated as change to wrong category consists of the entries where all three maps disagree, shown in green.

Figure of Merit

There is a plethora of possible summary parameters that could extract potentially enlightening information from the three-dimensional table, just as there is from a two-dimensional table. For example, it is possible to use the three-dimensional table to compute versions of the most popular two-dimensional parameters, such as overall accuracy, user's accuracy, producer's accuracy, kappa, and Pierce skill score (Congalton 1991; Fielding and Bell 1997; Stehman 1997, 1999). We focus on a measure called the *figure of merit*, which has become popular in geographic modeling (Klug et al. 1992; Pontius et al. 2007; Pontius et al. 2008) and is called the *critical success index* by atmospheric scientists (Jollife and Stephenson 2003). For our application to land change modeling, the figure of merit is the intersection of the observed change and simulated change divided by the union of the observed change and simulated change. Thus, it is a ratio that ranges from zero to one, where zero indicates no intersection between observed change and simulated change and one indicates perfect intersection between observed change and simulated change. None of the previously mentioned parameters

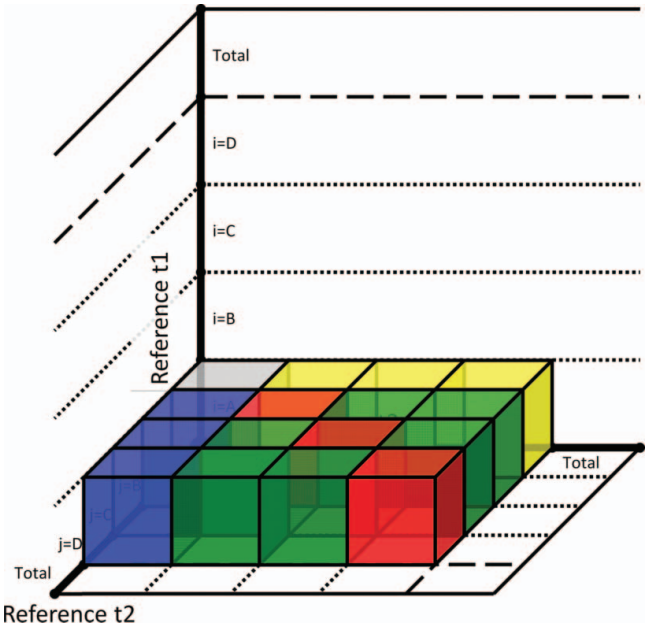

Figure 7. Entries that record transitions from category A of reference t1. Figure 7 is available in color online.

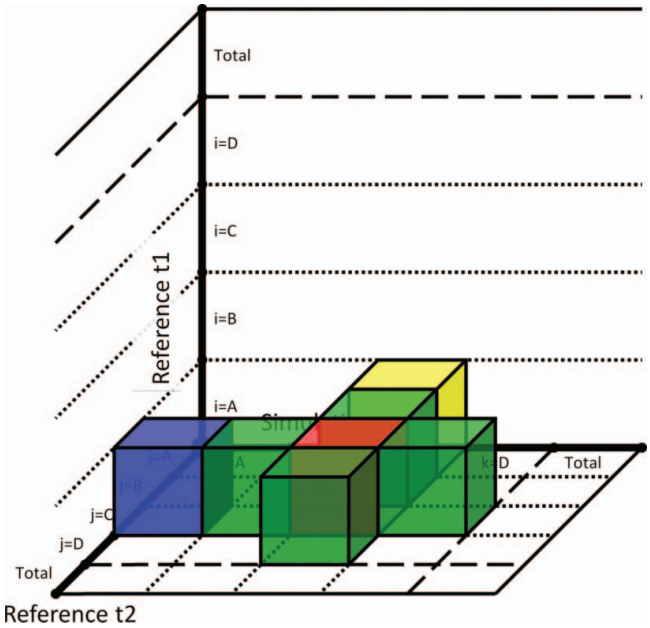

Figure 8. Entries that record observed or simulated transitions from category A at t1 to category C at t2. Figure 8 is available in color online.

have both of those properties. The figure of merit can be computed at a variety of levels. For our case study, three levels are particularly useful: (1) an overall level that measures the correspondence between any types of observed and simulated changes, (2) a category-specific level that measures the fate of a category in the reference t1 map, and (3) a transition-specific level that considers the transition between two specific categories.

Equation 9 gives the overall figure of merit for resolution g expressed as a percentage. The numerator computes the observed change that is simulated correctly, which is the sum of the entries in the vertical plane minus the persistence simulated correctly. The denominator computes the union of the observed change and simulated change, which is one minus the persistence simulated correctly.

$$F\bullet\bullet_g = \left(\frac{\sum_{i=1}^{J}\sum_{j=1}^{J} Uijj_g - \sum_{i=1}^{J} Uiii_g}{1 - \sum_{i=1}^{J} Uiii_g}\right) \times 100\% \tag{9}$$

Figure 7 shows the concept on which the figure of merit is based at a category-specific level for category A in reference t1. The persistence simulated correctly is in the single entry closest to the origin of the table. The other entries on the diagonal record changes simulated correctly from category A. Mathematically, Equation 10 gives the figure of merit for a transition from category i at resolution g, where the subtraction of $Uiii_g$ eliminates the correctly simulated persistence of category i.

$$Fi\bullet_g = \left(\frac{\sum_{j=1}^{J} Uijj_g - Uiii_g}{\sum_{j=1}^{J}\sum_{k=1}^{J} Uijk_g - Uiii_g}\right) \times 100\% \tag{10}$$

Figure 8 shows the concept on which the figure of merit is based at a transition-specific level, for a transition from A to C. Mathematically, Equation 11 gives the figure of merit for the transition from category i to j at resolution g. The first summation in the denominator computes the size of the observed transition from i to j and the second summation computes the size of the simulated transition from i to j. These two summations double count the transition from i to j that is simulated correctly, so we must subtract $Uijj_g$ once from the denominator.

$$Fij_g = \left(\frac{Uijj_g}{\sum_{k=1}^{J} Uijk_g + \sum_{k=1}^{J} Uikj_g - Uijj_g}\right) \times 100\% \tag{11}$$

Results

Figure 9 shows the results from an overlay of the three maps of Figure 1 for the Cho Don case study, summarized for two types of agreement and three types of disagreement. There is 54 percent overall agreement between reference 2001 and simulation 2001 at the 32-m resolution. The largest component is persistence simulated correctly, which is where all three maps match. The three-dimensional table indicates that the change simulated correctly consists almost entirely of two transitions: from crop to shrub and from shrub to forest. There is 46 percent disagreement between reference 2001 and simulation 2001, 31 percentage points of which are due to confusion between forest and shrub. The largest component of disagreement is change simulated as persistence, which is composed mainly of two observed transitions: from shrub to forest and from forest to shrub. The second largest component of disagreement is change simulated as change to wrong category, which is caused mostly by an observed change from crop to forest but simulated change from crop to shrub. The smallest component of disagreement is persistence simulated as change, which is composed mostly of observed persistence of shrub that is simulated to change to forest. Figure 9 shows that many of the various types of disagreements are intermingled spatially such that they are within a few pixels of each other.

The spatial proximity of the various types of disagreement influences the variation in the components of agreement and disagreement as resolution coarsens. Figure 10 gives the components and the overall figure of merit at multiple resolutions as the sides of the coarse squares grow by multiples of two. At a resolution of 32 km, two coarse squares distinguish the northern part from the southern part of the study area. At a resolution of 51 km, the entire study area resides in one coarse square. The bottom three components in Figure 10 constitute the observed change and the middle three components indicate simulated change. Overall disagreement shrinks from 46 percent at the 32-m resolution to 12 percent at the 32-km resolution to 3 percent at the 51-km resolution. This 3 percent disagreement at the coarsest resolution is quantity disagreement, meaning that it is attributable entirely to differences in the proportions of the categories in reference 2001 and simulation 2001 over the entire study area. Specifically, the table shows that there is more forest in reference 2001 than in simulation 2001. Quantity disagreement is constant across all resolutions, so the overwhelming majority of the disagreement at the 32-m resolution is attributable to allocation disagreement between reference 2001 and simulation 2001. The entries in the three-dimensional table reveal that overall agreement grows as resolution becomes slightly coarser because disagreement due to change simulated as persistence becomes persistence simulated correctly. This is attributable to close spatial proximity between (1) pixels that show a reference transition from shrub to forest but are simulated as persistence and (2) pixels that show a reference transition from forest to shrub but are simulated as persistence. Figure 10 also shows that change simulated correctly becomes persistence simulated correctly as resolution becomes slightly coarser. This is attributable to close spatial proximity between (1) pixels that show change simulated correctly from shrub to forest and (2) pixels that show change simulated correctly from forest to shrub. Between resolutions of 32 m and 32 km, disagreement due to change simulated as change to wrong category remains larger than 6 percent. This component of disagreement then becomes change simulated correctly at a resolution of 51 km, which indicates that the disagreement is due to spatial misallocation between north and south. The table's entries reveal that the main reason is that the northern part of reference 2001 has more forest and less shrub than the northern part of simulation 2001, whereas the southern part of reference 2001 has more shrub and less forest than the southern part of simulation 2001. Consequently, the overall figure of merit varies between 18 percent and 30 percent at resolutions between 32 m and 32 km and then spikes to 78 percent at a resolution of 51 km.

When we examine a single layer of entries within the three-dimensional table, we see how the gross loss of the crop category of 1990 is associated with important aspects of the variation in the overall results that Figure 10 shows. Figure 11 illustrates the fate of the 1990 crop category by showing the categories in the 2001 reference and simulation maps for pixels that were crop in 1990. The reference maps show that forest gains the most from crop, whereas the simulation shows that shrub gains the most from crop.

Figure 12 gives the components of change and the category-specific figure of merit at multiple resolutions for the area in 1990 that is crop, which constitutes 19 percent of the study area. Crop is the category that experiences the largest net quantity change according to the observed and simulated changes. Figure 12 shows how resolution influences the distribution of the types of transitions. Disagreement becomes change simulated correctly as resolution coarsens from 32 km to 51 km.

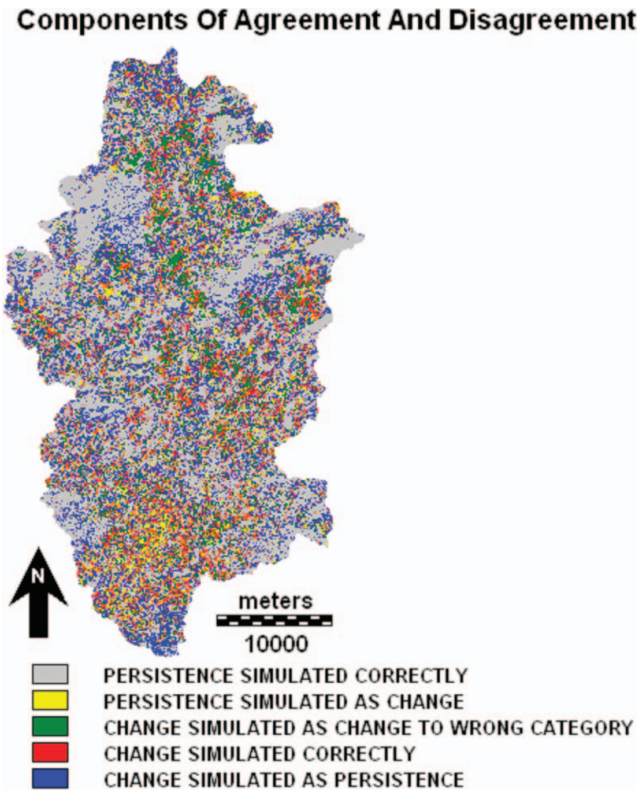

Figure 9. Map of components of agreement and disagreement at 32-m resolution.

The category-specific figure of merit is close to 30 percent at nearly all resolutions and then increases substantially between resolutions of 32 km and 51 km as the allocation disagreement between north and south becomes resolved. At an even more detailed level, the entries within in the crop layer of the three-dimensional table allow us to see that the particular transition from crop to shrub is responsible for most of the variation in Figure 12. Figure 13 gives the components of change and the figure of merit at multiple resolutions for the transition from crop to shrub, which is the largest simulated transition, accounting for 14 percent of the study area at the 32-m resolution. The transition-specific figure of merit for the transition from crop to shrub shows a pattern of variation with resolution that is similar to the figure of merit for crop of 1990 (Figure 12) and for overall change (Figure 11). These results reflect the model's assumption that crop transitions to shrub throughout the entire study area, whereas the reference maps reveal that crop transitions mainly to forest, particularly in the north compared to the south.

Figure 14 shows the reference and simulation categories of 2001 for the pixels that were shrub in 1990. The reference map shows that most of the 1990 shrub

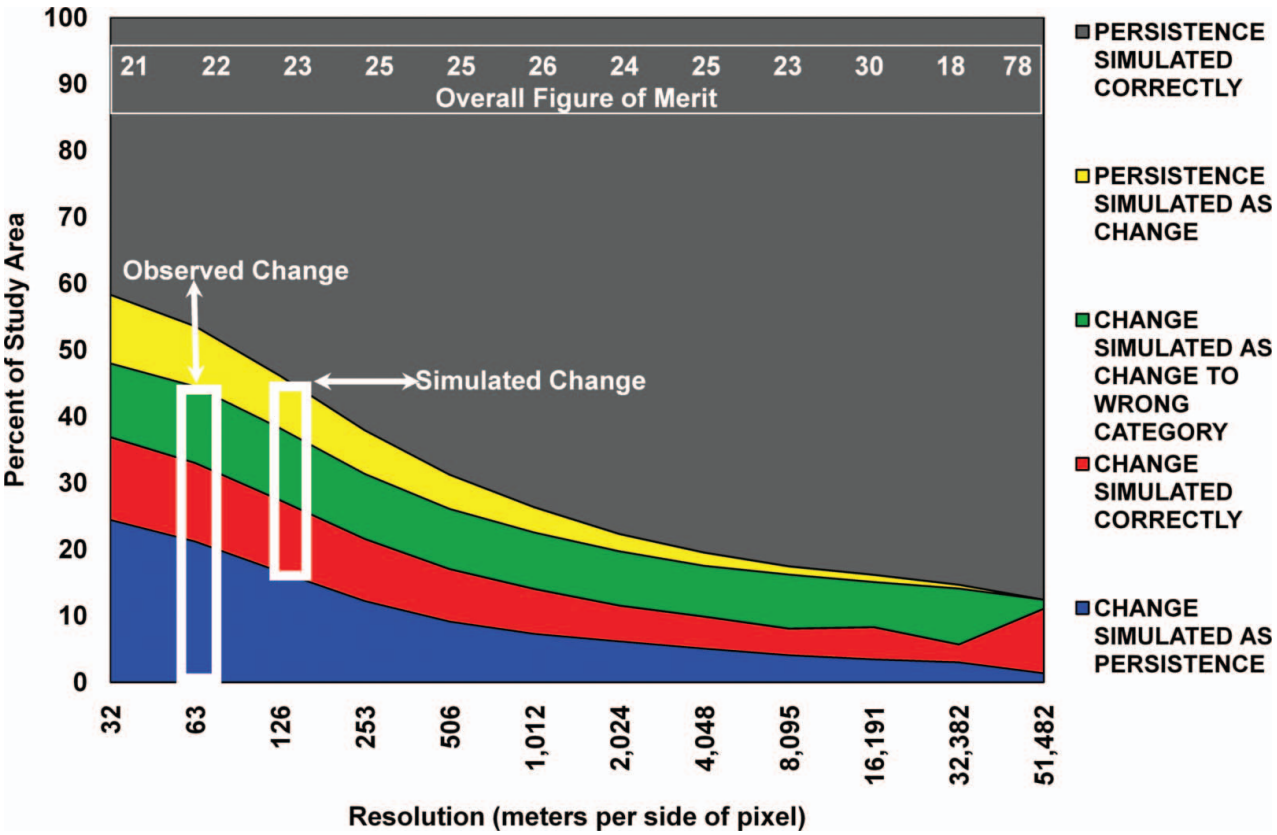

Figure 10. Components of agreement and disagreement for the entire study area at multiple resolutions with the associated overall figure of merit.

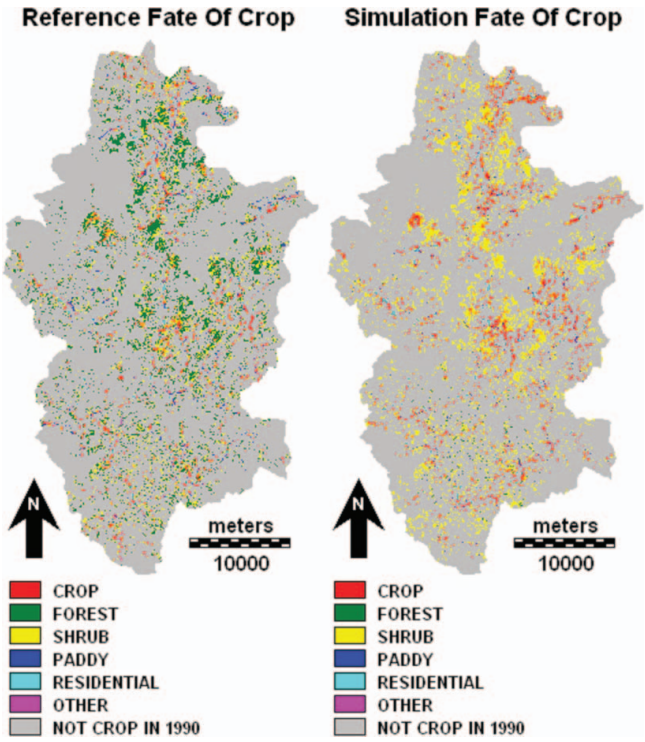

Figure 11. Maps of observed and simulated categories that transition from 1990 crop. Figure 11 is available in color online.

transitions to forest, whereas the simulation map shows that most of the 1990 shrub persists as shrub. The northern part of the study area shows a larger reference transition from shrub to forest than the simulation transition from shrub to forest, whereas the southern part of the study area shows just the opposite, i.e., a smaller reference transition to forest than the simulation transition. This is a major reason for the differences between reference 2001 and simulation 2001 with respect to the allocation of shrub and forest between north and south.

Discussion

A substantial portion of the overall disagreement is attributable to minor allocation disagreement, which is the amount by which disagreement shrinks during the conversion from the native resolution to a coarser resolution. We expect minor allocation disagreement to exist in the simulation map because the rules of the SAMBA multiagent model are designed mainly to simulate the quantity of each land transition at the village level and are not necessarily meant to locate precisely where the changes occur within a village. In

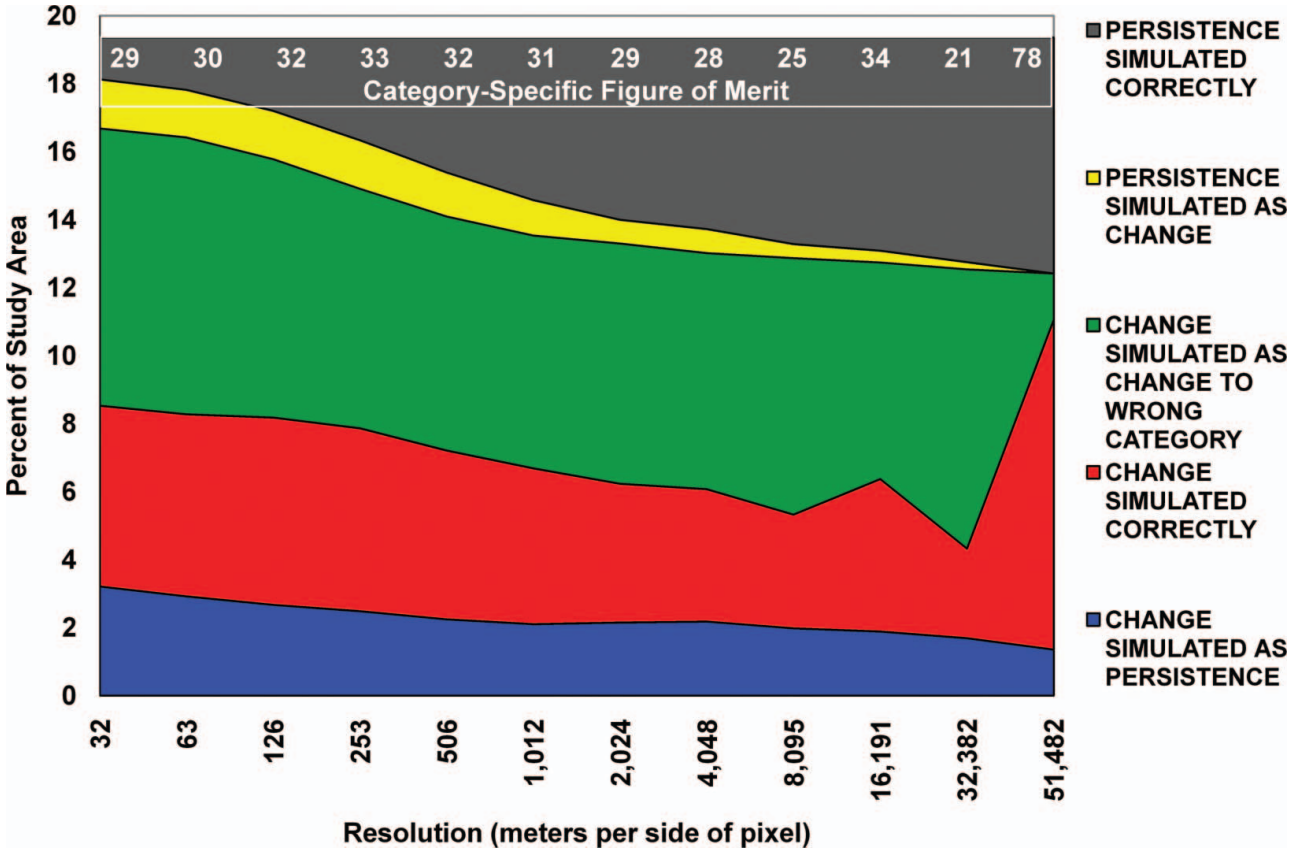

Figure 12. Components of agreement and disagreement for transitions from crop at multiple resolutions with the associated category-specific figure of merit. Figure 12 is available in color online.

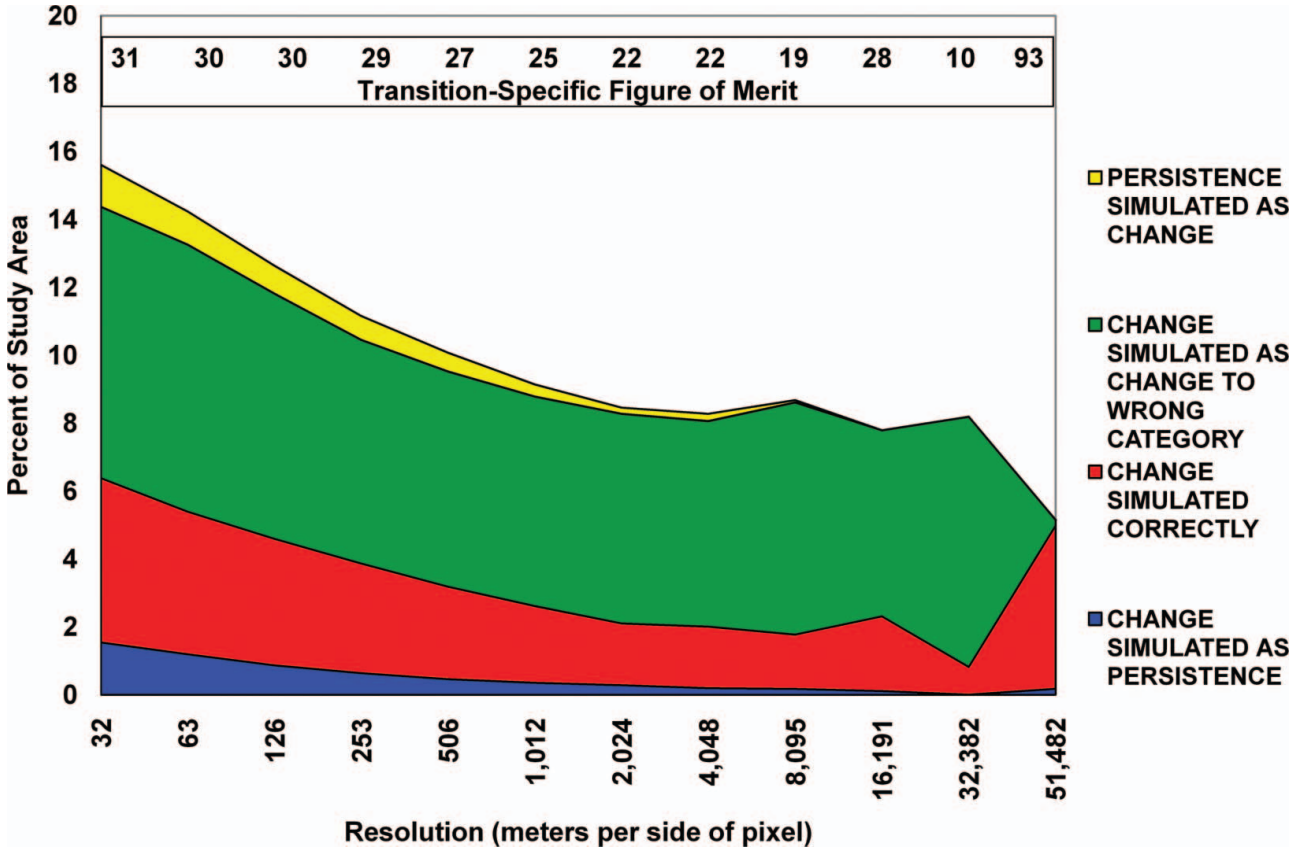

Figure 13. Components of agreement and disagreement for the transition from crop to shrub at multiple resolutions with the associated transition-specific figure of merit. Figure 13 is available in color online.

the simulation, each household selects pixels randomly from among the pixels that match the household's criteria for land conversion. These criteria can depend on the household's land use strategies (e.g., proximity to house) and on particular crop requirements (e.g., fertility of soil, angle of slope, distance to stream). So the simulation map should be judged by the quantities of the transitions that occur in a village and by the general patterns of land change, not by the exact allocation of the converted pixels at the 32-m resolution. Half of the disagreement at the 32-m resolution is allocation disagreement that occurs within squares that are 506 m × 506 m. The size of these squares corresponds approximately to the average size of a village in Cho Don District; therefore this minor allocation disagreement is close enough to be considered agreement for practical purposes of the modeling project. Consequently, the simulation demonstrates how policies that influence households can explain land conversions at the village scale. These results are consistent with the hypothesis that land reforms transformed regional landscapes by altering management at the village level, not by planning at higher levels.

Nine percentage points of overall disagreement are attributable to major allocation disagreement between the northern and southern parts of the study area with respect to forest and shrub. The north and south are different with respect to soil, geomorphology, and climate; thus, forest regeneration is faster in the north than in the south, as farmers confirmed through interviews and participatory simulations (Castella 2009). Abandoned cropland tends to transition mostly to forest in the north, whereas abandoned cropland tends to transition more to shrub in the south. The model uses a single parameterization for the entire study area concerning the speed of forest regeneration, so the simulation misses this difference in physical geography between north and south. The model would need to use different sets of parameters in the north versus the south to capture this difference. The multiple-resolution analysis allows us to measure the effect of the model's incorrect assumption concerning forest regeneration parameters across space.

Most of the disagreement at the native resolution between reference 2001 and simulation 2001 is attributable to confusion between forest and shrub. This raises questions about the definitions of the land

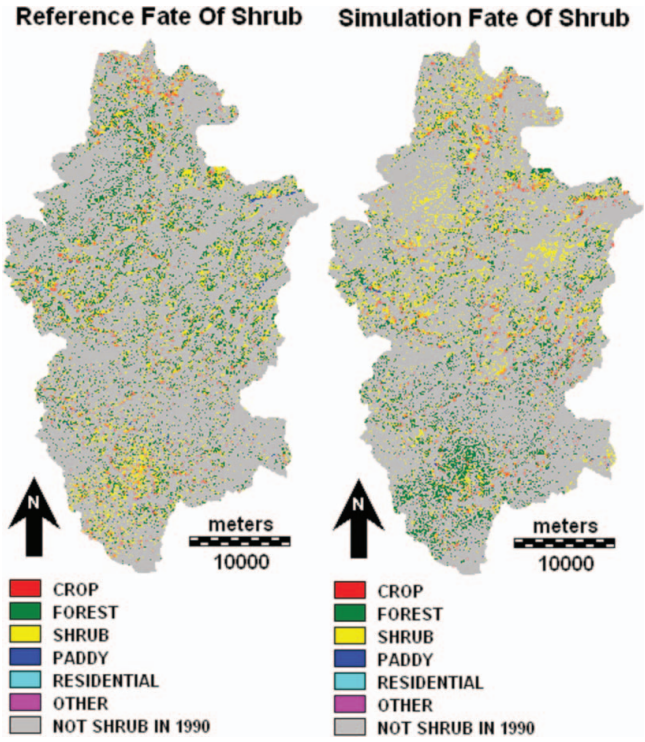

Figure 14. Maps of observed and simulated categories that transition from 1990 shrub. Figure 14 is available in color online.

categories, because the practical distinction between forest and shrub is blurred, even in the reference maps. Therefore, we need to consider uncertainty from two possible sources: the model and the reference maps (Pontius and Petrova 2010). It was difficult to distinguish forest from shrub during the construction of the reference maps, which derived from interpretation of satellite images. Some of the disagreement among the three maps might derive from errors in the reference data. If errors in the reference maps were to manifest as minor allocation disagreement at resolutions that are slightly coarser than the native resolution, then our method would treat those errors as agreement. If errors in the reference maps were to manifest as quantity disagreement, however, our method would treat those errors as disagreement at all resolutions. The multiple-resolution method is well adapted to the Cho Don case study and the purpose of the SAMBA model because the method allows interpretation of various types of disagreement, whether the disagreement is generated by the model's rules or by the reference maps.

Some readers might be tempted to ask, "Is the level of agreement acceptable?" An answer to this question would require a definition of *acceptable*. Pontius et al. (2008) examined thirteen applications of land change models and found that the overall figure of merit ranged from 1 percent to 59 percent. They also discovered that examination of the types of agreement and disagreement was useful, even without giving a universal definition of acceptable. It does not make sense to have a universal standard for acceptability, because any definition should relate to the particular goal of the modeling application, and different applications have different goals (Pontius et al. 2007). The application of SAMBA to Cho Don District did not have a goal to attain a particular level of accuracy. A main goal was to attain insight concerning how the observed transitions correspond to the simulated transitions. The multiple-resolution method satisfies this goal because the method interprets each entry in the three-dimensional table as the proportion of the study area that has a particular combination of categories in the three maps, and the method computes the table in a manner that differentiates minor allocation disagreement from major allocation disagreement from quantity disagreement. In this sense, the results are acceptable because they reveal important information, which is what the method was designed to do.

The next step in the development of this method is to examine additional meaningful ways to modify the areal units. Our multiple-resolution algorithm modifies the areal units in a systematic manner by computing a sequence of nested square partitions. The statistical results concerning map comparison can vary substantially depending on how the areal units are modified; thus, this is a case of the modifiable areal unit problem. We do not see this characteristic as a problem; we see it as an opportunity to learn about the maps. The variation in results across larger areal units indicates the spatial allocation of the disagreement among the modified areal units. For proper interpretation, users need to consider how the modified areal units partition the study area. For example, the 32-km coarse squares partition this article's case study in a manner that compares the north to the south, which is important for interpretation in Cho Don, Vietnam.

There might be additional ways to partition the landscape into modified areal units that would facilitate even deeper interpretation. For example, Pontius et al. (2007) used a map of household parcel boundaries to partition their study area into coarser areal units that are meaningful to the process of land transformation in the Amazon basin. For their application, the pixels within coarser household parcels are aggregated, so minor allocation disagreement means allocation disagreement within a household parcel. This type of stratification is helpful when investigators want to ignore the pixel-level allocation disagreement within larger areal strata, such as household parcels, census tracks, or political

units. Pontius et al. (2007) and Pontius, Thontteh, and Chen (2008) presented equations for using a map of strata to partition the study area for a two-map comparison. This article's equations for a three-map comparison can be applied in an identical manner for cases where there exists a map of meaningful strata for partitioning. Our equations for the three-dimensional table can be used for any partitioning of the study area, even when the strata are nonsquare, of nonequal area, and noncontiguous, because our equations have a weight (Wn_g) to account for the size of each coarse stratum (n_g). For the case study in Vietnam, we are interested in the general spatial allocation of disagreement; therefore, it is helpful to use a multiple-resolution algorithm that produces a sequence of nested coarse squares.

Conclusions

This article presents a method to compare observed versus simulated transitions among land categories by comparing three maps: reference t1, reference t2, and simulation t2. The method considers multiple resolutions by computing a three-dimensional table for cases where the maps' areal units contain proportions of more than one category. The three-dimensional table quantifies simultaneously the observed and simulated transitions among categories. Furthermore, the multiple-resolution analysis reveals information that analysis at a single resolution cannot reveal, because the three-dimensional table differentiates minor allocation disagreement within coarse squares from major allocation disagreement among coarse squares. The method produces results that allow for important insights concerning the observed land change processes and the behavior of the simulation model. We encourage our colleagues to use this approach to shed light on how variation in scale influences statistical measurements in the context of spatially explicit dynamic modeling.

Acknowledgments

The SAMBA model and land use maps from Cho Don District were developed within the framework of the Mountain Agrarian Systems Project by the Vietnam Academy of Agricultural Sciences, the International Rice Research Institute, and the Institut de Recherche pour le Développement. The authors thank all the colleagues involved in this project for their contribution to the maps that illustrate the method presented in this article. Clark University's School of Geography and Department of International Development, Community, and Environment awarded a scholarship for the second author to earn a master's degree, allowing her to contribute to this article's research. We also thank anonymous reviewers whose comments helped to improve this article.

References

Alo, C., and R. G. Pontius, Jr. 2008. Identifying systematic land cover transitions using remote sensing and GIS: The fate of forests inside and outside protected areas of Southwestern Ghana. *Environment and Planning B* 35 (2): 280–95.

Atkinson, P. M., and N. J. Tate. 2000. Spatial scale problems and geostatistical solutions: A review. *The Professional Geographer* 52 (4): 607–23.

Bian, L. 1997. Multiscale nature of spatial data in scaling up environmental models. In *Scale in remote sensing and GIS*, ed. D. Quattrochi and M. Goodchild, 13–26. Boca Raton, FL: CRC Press.

Binaghi, E., P. Brivio, P. Ghezzi, and A. Rampini. 1999. A fuzzy set-based accuracy assessment for soft classification. *Pattern Recognition Letters* 20:935–48.

Cao, C., and N. Lam. 1997. Understanding the scale and resolution effects in remote sensing and GIS. In *Scale in remote sensing and GIS*, ed. D. Quattrochi and M. Goodchild, 57–72. Boca Raton, FL: CRC Press.

Castella, J.-C. 2009. Assessing the role of learning devices and geovisualisation tools for collective action in natural resource management: Experiences from Vietnam. *Journal of Environmental Management* 90:1313–19.

Castella, J.-C., S. Boissau, N. H. Thanh, and P. Novosad. 2006. Impact of forestland allocation on land use in a mountainous province of Vietnam. *Land Use Policy* 23 (2): 147–60.

Castella, J.-C., S. Boissau, T. N. Trung, and D. D. Quang. 2005. Agrarian transition and lowland–upland interactions in mountain areas in northern Vietnam: Application of a multi-agent simulation model. *Agricultural Systems* 86 (3): 312–32.

Castella, J.-C., N. R. Tronche, and V. Nguyen. 2002. Landscape changes in *Cho Don* District during the *doi moi* era (1990–2000) and their implications for sustainable natural resource management in *Viet Nam*'s mountainous provinces. In *Doi Moi in the mountains: Land use changes and farmers' livelihood strategies in Bac Kan Province, Viet Nam*, ed. J.-C. Castella and D. D. Quang, 149–73. Ha Noi, Vietnam: The Agricultural Publishing House.

Castella, J.-C., T. N. Trung, and S. Boissau, S. 2005. Participatory simulation of land-use changes in the northern mountains of Vietnam: The combined use of an agent-based model, a role-playing game, and a geographic information system. *Ecology and Society* 10 (1): 27. http://www.ecologyandsociety.org/vol10/iss1/art27/ (last accessed 23 September 2010).

Collins, J. B., and C. E. Woodcock. 1999. Geostatistical estimation of resolution-dependent variance in remotely sensed images. *Photogrammetric Engineering and Remote Sensing* 65 (1): 41–51.

Congalton, R. G. 1991. A review of assessing the accuracy of classifications of remotely sensed data. *Remote Sensing of Environment* 37:35–46.

Congalton, R. G., and K. Green. 1999. *Assessing the accuracy of remotely sensed data: Principles and practices*. New York: Lewis.

Csillag, F., and B. Boots. 2006. Special issue—Categorical map comparison. *Journal of Geographical Systems* 8 (2): 109–226.

Dietzel, C. K., and K. C. Clarke. 2004. Spatial differences in multi-resolution urban automata modeling. *Transactions in GIS* 8:479–92.

Fielding, A. H., and J. F. Bell. 1997. A review of methods for the assessment of prediction errors in conservation presence/absence models. *Environmental Conservation* 24 (1): 38–49.

Fisher P., C. Arnot, R. Wadsworth, and J. Wellens. 2006. Detecting change in vague interpretations of landscapes. *Ecological Informatics* 1 (2): 167–78.

Foody, G. M. 2002. Status of land cover classification accuracy assessment. *Remote Sensing of Environment* 80:185–201.

Gómez, D., G. Biging, and J. Montero. 2008. Accuracy statistics for judging soft classifications. *International Journal of Remote Sensing* 29 (3): 683–709.

Goodchild, M. F., and D. A. Quattrochi. 1997. Introduction: Scale, multiscaling, remote sensing, and GIS. In *Scale in remote sensing and GIS*, ed. D. Quattrochi and M. Goodchild, 1–12. Boca Raton, FL: CRC Press.

Jollife, I. T., and D. B. Stephenson. 2003. *A practitioner's guide in atmospheric science*. Hoboken, NJ: Wiley.

Klug, W., G. Graziani, G. Grippa, D. Pierce, and C. Tassone, eds. 1992. *Evaluation of long range atmospheric transport models using environmental radioactivity data from the Chernobyl accident: The ATMES report*. London: Elsevier.

Kuzera, K., and R. G. Pontius, Jr. 2008. Importance of table construction for multiple-resolution categorical map comparison. *GIS and Remote Sensing* 45 (3): 249–74.

Lam, N., D. Catts, D. Quattrochi, D. Brown, and R. McMaster. 2004. Scale. In *A research agenda for geographic information science*, ed. R. McMaster and L. Usery, 93–128. Boca Raton, FL: CRC Press.

Latifovic, R., and I. Olthof. 2004. Accuracy assessment using sub-pixel fractional error matrices of global land cover products derived from satellite data. *Remote Sensing of Environment* 90:153–65.

Lewis, H. G., and M. Brown. 2001. A generalized confusion table for assessing area estimates from remotely sensed data. *International Journal of Remote Sensing* 22:3223–35.

Marceau, D. J. 1999. The scale issue in social and natural sciences. *Canadian Journal of Remote Sensing* 25 (4): 347–56.

Meyfroidt, P., and E. F. Lambin. 2008. Forest transition in Vietnam and its environmental impacts. *Global Change Biology* 14 (6): 1319–36.

Okeke, F., and A. Karnieli. 2006. Methods for fuzzy classification and accuracy assessment of historical aerial photographs for vegetation change analyses. Part I: Algorithm development. *International Journal of Remote Sensing* 27 (1–2): 153–76.

Openshaw, S. 1984. *The modifiable areal unit problem*. Norwich, UK: GeoBooks.

Pontius, R. G., Jr. 2002. Statistical methods to partition effects of quantity and location during comparison of categorical maps at multiple resolutions. *Photogrammetric Engineering & Remote Sensing* 68 (10): 1041–49.

Pontius, R. G., Jr., W. Boersma, J. C. Castella, K. Clarke, T. de Nijs, C. Dietzel, Z. Duan et al. 2008. Comparing the input, output, and validation maps for several models of land change. *Annals of Regional Science* 42 (1): 11–47.

Pontius, R. G., Jr., and M. L. Cheuk. 2006. A generalized cross-tabulation table to compare soft-classified maps at multiple resolutions. *International Journal of Geographical Information Science* 20 (1): 1–30.

Pontius, R. G., Jr., and J. Connors. 2009. Range of categorical associations for comparison of maps with mixed pixels. *Photogrammetric Engineering & Remote Sensing* 75 (8): 963–69.

Pontius, R. G., Jr., D. Huffaker, and K. Denman. 2004. Useful techniques of validation for spatially explicit land-change models. *Ecological Modelling* 179 (4): 445–61.

Pontius, R. G., Jr., and S. Petrova. 2010. Assessing a predictive model of land change using uncertain data. *Environmental Modelling & Software* 25 (3): 299–309.

Pontius, R. G. Jr., O. Thontteh, and H. Chen. 2008. Components of information for multiple resolution comparison between maps that share a real variable. *Environmental and Ecological Statistics* 15 (2): 111–42.

Pontius, R. G. Jr., R. Walker, R. Yao-Kumah, E. Arima, S. Aldrich, M. Caldas, and D. Vergara. 2007. Accuracy assessment for a simulation model of Amazonian deforestation. *Annals of the Association of American Geographers* 97 (4): 677–95.

Silván-Cárdenas, J. L., and L. Wang. 2008. Sub-pixel confusion-uncertainty for assessing soft classifications. *Remote Sensing of Environment* 112:1081–95.

Stehman, S. V. 1997. Selecting and interpreting measures of thematic classification accuracy. *Remote Sensing of Environment* 62:77–89.

———. 1999. Comparing thematic maps based on map value. *International Journal of Remote Sensing* 20 (12): 2347–66.

Stehman, S. V., M. K. Arora, T. Kasetkasem, and P. K. Varshney. 2007. Estimation of fuzzy error table accuracy measures under stratified random sampling. *Photogrammetric Engineering & Remote Sensing* 73 (2): 165–73.

Townsend, P. A. 2000. A quantitative fuzzy approach to assess mapped vegetation classifications for ecological applications. *Remote Sensing of Environment* 72:253–67.

Visser, H., and T. de Nijs. 2005. The map comparison kit. *Environmental Modelling & Software* 21:346–58.

Woodcock, C., and S. Gopal. 2000. Fuzzy set theory and thematic maps: Accuracy assessment and area estimation. *International Journal of Geographic Information Science* 14:153–72.

Wu, J. 2004. Effects of changing scale on landscape pattern analysis: Scaling relations. *Landscape Ecology* 19:125–38.

Correspondence: Clark University, School of Geography, Worcester, MA 01610, e-mail: rpontius@clarku.edu (Pontius); Mactec Engineering and Consulting, Oakland, CA 94610, e-mail: smitha.peethambaram@gmail.com (Peethambaram); Institut de Recherche pour le Développement (IRD, France) and Centre for International Forestry Research (CIFOR, Indonesia), P.O. Box 5992, Vientiane, Lao PDR, e-mail: j.castella@ird.fr (Castella).